

## LETTER

**Hydrology, rather than wildfire burn extent, determines post-fire organic and black carbon export from mountain rivers in central coastal California**Riley Barton<sup>1\*</sup>, Christina M. Richardson<sup>2</sup>, Evelyn Pae<sup>1</sup>, Maya S. Montalvo<sup>2,3</sup>, Michael Redmond<sup>2,4</sup>, Margaret A. Zimmer<sup>2a</sup>,  
Sasha Wagner<sup>1\*</sup><sup>1</sup>Department of Earth and Environmental Sciences, Rensselaer Polytechnic Institute, Troy, New York, USA; <sup>2</sup>Department of Earth and Planetary Sciences, University of California, Santa Cruz, California, USA; <sup>3</sup>Department of Geography, Simon Fraser University, Burnaby, British Columbia, Canada; <sup>4</sup>Department of Climate and Space Sciences and Engineering, University of Michigan at Ann Arbor, Ann Arbor, Michigan, USA**Scientific Significance Statement**

Fires in coastal mountain watersheds alter the quantity and quality of organic carbon, including fire-derived black carbon (BC), exported to the ocean. The relationship between terrestrial wildfire characteristics and post-burn carbon fluxes is poorly constrained, making it difficult to predict fire-induced perturbations to aquatic carbon cycling and overall water quality. This study shows that, 1-yr post-fire, BC export from different coastal mountain rivers affected by the 2020 CZU Lightning Complex Fires (California, USA) was primarily driven by hydrology rather than percentage of drainage area burned.

**Abstract**

Coastal mountain rivers export disproportionately high quantities of terrestrial organic carbon (OC) directly to the ocean, feeding microbial communities and altering coastal ecology. To better predict and mitigate the effects of wildfires on aquatic ecosystems and resources, we must evaluate the relationships between fire, hydrology, and carbon export, particularly in the fire-prone western United States. This study examined the spatiotemporal export of particulate and dissolved OC (POC and DOC, respectively) and particulate and dissolved black carbon (PBC and DBC, respectively) from five coastal mountain watersheds following the 2020 CZU Lightning Complex Fires (California, USA). Despite high variability in watershed burn extent (20–98%),

\*Correspondence: bartor2@rpi.edu; wagnes3@rpi.edu

<sup>a</sup>Present address: U.S. Geological Survey Upper Midwest Water Science Center, Madison, Wisconsin, USA**Associate editor:** Henrietta Dulai

**Author Contribution Statement:** CMR, MAZ, and SW came up with the research question and designed the study approach. CMR, MR, and MSM collected and prepared all field samples. CMR and MR conducted all POC, absorbance, and geographical analyses. RB and EP conducted DOC, DBC, and PBC analyses. RB performed all statistical analyses and led the interpretation of the data. RB led the writing of the manuscript with contributions from all authors.

**Data Availability Statement:** Data are available in the CUAHSI Hydroshare data repository <https://doi.org/10.4211/hs.94fb3a67a74a48c9a89dda8046fdb2df>.

Additional Supporting Information may be found in the online version of this article.

This is an open access article under the terms of the [Creative Commons Attribution](#) License, which permits use, distribution and reproduction in any medium, provided the original work is properly cited.

annual POC, DOC, PBC, and DBC concentrations remained relatively stable among the different watersheds. Instead, they correlated significantly with watershed discharge. Our findings indicate that hydrology, rather than burn extent, is a primary driver of post-fire carbon export in coastal mountain watersheds.

The burning of organic matter via wildfire produces pyrogenic carbon, representing a combustion continuum of molecules whose chemical properties depend on fuel type and burn conditions (Masiello 2004; Coppola et al. 2022). Black carbon (BC) is the condensed aromatic fraction of pyrogenic carbon that is formed at high charring temperatures (Schneider et al. 2010), resistant to microbial degradation (Kuzakov et al. 2014), highly photolabile (Stubbins et al. 2012), and considered a net carbon sink (Jones et al. 2019). Although the majority of global BC is produced from fire (Coppola et al. 2022), condensed aromatic molecules are also present in oil (Goranov et al. 2021; Podgorski et al. 2021) and fossil fuel combustion products (Bond et al. 2013). BC is ubiquitous and exists as part of bulk organic carbon (OC) in terrestrial and aquatic environments (Goldberg 1985). During hydrologic events, OC and associated BC are mobilized from the burned landscape to lower reaches of the watershed and downstream waterbodies (e.g., lakes and oceans), thereby affecting downstream water quality (Shakesby et al. 2016). The increased mobilization of sediment, OC, and BC post-fire can also pose challenges for downstream water resources and treatment facilities (Cawley et al. 2017; Robinne et al. 2018, 2021; Hohner et al. 2019; Chen et al. 2022).

The hydrological and biogeochemical responses of a watershed to wildfire are specific to both catchment and fire conditions (Nunes et al. 2018), with catchment conditions often altered post-fire (Shakesby and Doerr 2006). For example, increased burn severity increases soil hydrophobicity, changing hydrologic flow paths and causing increased runoff, erosion, and flooding risks (Shakesby et al. 2000; Shakesby and Doerr 2006). While interconnected, fire- and catchment-specific drivers of OC and BC transport post-fire vary depending on the organic matter's molecular makeup or size. The transfer of particulate material, including particulate BC and OC (PBC and POC, respectively), from the hillslope to the stream channel is primarily driven by erosional processes, with mobilization linked to precipitation events, snowmelt, and periods of overland flow (Galy et al. 2015; Cotrufo et al. 2016; Coppola et al. 2022). Post-fire hydrologic events can also lead to increased total suspended solids (TSS) concentrations, as fires destabilize soil and remove vegetation (Hohner et al. 2019). Consequentially, the export of PBC is often coupled with the export of TSS in fire-affected watersheds (Wagner et al. 2015; Cotrufo et al. 2016; Coppola et al. 2018). Catchment slope and geomorphology have been shown to influence PBC mobility, but fire severity results in the preferential erosion of charcoal from the hillslope, and is thus considered a primary driver of PBC export in recently burned watersheds (Abney et al. 2019).

Factors controlling the post-fire mobilization of dissolved organic constituents are less clear. Dissolved OC (DOC) concentrations have been observed to increase, decrease, or remain consistent in aquatic systems post-fire (Jensen et al. 2017; Hohner et al. 2019; Uzun et al. 2020; Wei et al. 2021), with greater variability observed in smaller streams (Raoelison et al. 2023). Overall, riverine DOC concentrations tend to be slightly higher after a burn event (Raoelison et al. 2023). The riverine export of condensed aromatic dissolved BC (DBC), which is a hydrophobic molecular class, is driven by solubility (Wagner et al. 2018). Therefore, some degree of oxidation is required to enhance its polarity and aqueous mobility (Abiven et al. 2011; Coppola et al. 2022). This solubility requirement may explain the strong coupling of DOC and DBC export in fire-affected rivers (Wagner et al. 2018) and the lack of apparent relationship between DBC concentration and fire history in some systems (Ding et al. 2013).

Fire activity is predicted to increase in regions experiencing regular drought periods and high fuel drying trends (Bowman et al. 2020; Ellis et al. 2022). In California, USA, wildfire frequency and severity has increased fivefold over the last four decades (Williams et al. 2019). Coastal fires are of particular concern as regional mountain rivers facilitate rapid and direct inputs of terrestrial carbon and nutrient subsidies to marine environments (Masiello and Druffel 2001; Hunsinger et al. 2008). The impacts of wildfire on water quality, watershed carbon export, and coastal food webs are poorly constrained, limiting our capacity to accurately predict and mitigate them. Here, we examined BC and OC export from five small coastal mountain watersheds which burned during the 2020 CZU Lightning Complex Fires (California, USA). All samples were collected during the first post-fire water year. The main objectives of this research were to (1) determine whether burn extent was a primary control on BC and OC mobilization, (2) evaluate temporal variations between DOC and DBC concentrations, and (3) examine BC and OC export from coastal mountain rivers across various flow conditions.

## Methods

### Study location

We sampled five adjacent watersheds of varying catchment sizes (9–276 km<sup>2</sup>; Table 1) in the Santa Cruz Mountains (California, USA): the San Lorenzo River and the Laguna, Pescadero, Majors, and Scott creeks. The portion of these basins that drains to the sampling locations (Fig. 1) is in a Mediterranean climate region. There, precipitation occurs mostly in winter as rain (700–1160 mm annually) and watersheds are dominated by evergreen and mixed forests

**Table 1.** Stream characteristics from the 1<sup>st</sup> water year post-fire. Area and burn extent values are representative of the subsection of watershed captured by sampling. Values presented for POC, DOC, PBC, DBC, PBC : DOC ratios, and particulate and dissolved BC molecular marker concentrations (pBPCA and dBPCA, respectively), and particulate and dissolved B6CA : B5CA ratios (pB6CA : B5CA and dB6CA : B5CA, respectively) are averages  $\pm$  standard deviation.

Watershed	Area (km <sup>2</sup> )	Burn extent (%)	POC (mg C L <sup>-1</sup> )	PBC (mg C L <sup>-1</sup> )	PBC : POC (%)	DOC (mg C L <sup>-1</sup> )	DBC (mg C L <sup>-1</sup> )	DBC : DOC (%)	pB6CA (nM)	pB5CA (nM)	pB6CA : B5CA	dB6CA (nM)	dB5CA (nM)	dB6CA : B5CA
San Lorenzo River	276	20	6.04 $\pm$ 8.97	0.19 $\pm$ 0.35	1.99 $\pm$ 1.11	4.83 $\pm$ 2.70	0.20 $\pm$ 0.11	4.23 $\pm$ 1.13	154 $\pm$ 289	166 $\pm$ 315	1.00 $\pm$ 0.09	84.4 $\pm$ 58.7	211 $\pm$ 126	0.39 $\pm$ 0.04
Pescadero Creek	118.7	23	0.75 $\pm$ 0.60	0.01 $\pm$ 0.01	1.78 $\pm$ 1.44	3.87 $\pm$ 0.81	0.20 $\pm$ 0.05	5.10 $\pm$ 0.81	5.08 $\pm$ 5.39	6.38 $\pm$ 6.38	0.81 $\pm$ 0.07	80.6 $\pm$ 26.9	212 $\pm$ 52	0.38 $\pm$ 0.04
Majors Creek	9.9	37	3.54 $\pm$ 6.08	0.09 $\pm$ 0.17	3.50 $\pm$ 1.88	4.10 $\pm$ 3.35	0.17 $\pm$ 0.16	3.96 $\pm$ 1.05	71.7 $\pm$ 140	71.4 $\pm$ 139	0.97 $\pm$ 0.04	80.5 $\pm$ 83.2	171 $\pm$ 176	0.46 $\pm$ 0.04
Laguna Creek	9	60	2.37 $\pm$ 3.99	0.06 $\pm$ 0.10	4.64 $\pm$ 3.09	4.11 $\pm$ 2.29	0.15 $\pm$ 0.09	3.75 $\pm$ 1.04	45.7 $\pm$ 83.6	44.2 $\pm$ 81.7	1.00 $\pm$ 0.06	66.1 $\pm$ 41.8	157 $\pm$ 97	0.43 $\pm$ 0.05
Scott Creek	73.5	98	4.94 $\pm$ 10.6	0.15 $\pm$ 0.29	3.53 $\pm$ 2.68	3.23 $\pm$ 1.82	0.14 $\pm$ 0.07	4.76 $\pm$ 1.55	110 $\pm$ 222	130 $\pm$ 268	0.87 $\pm$ 0.08	57.3 $\pm$ 33.4	149 $\pm$ 88	0.38 $\pm$ 0.01

(80–93%) with average slopes ranging from 21.4 to 35.6% (as determined using ArcGIS; Supplementary Table S1). These watersheds, which serve as drinking water sources to surrounding communities, burned to various extents (20–98% of total catchment area) during the CZU Lightning Complex Fires from 16 August 2020 to 22 September 2020 (Fig. 1). Prior to 2020, these watersheds experienced little fire activity with only five small fires (1–31 km<sup>2</sup>) occurring from 1950 to 2019 (Supplementary Fig. S1). In comparison, the 2020 CZU Lightning Complex Fires burned much larger (>350 km<sup>2</sup>) and more intensely. Due to storm-induced inaccessibility to the sampling site, two high flow samples for Scott Creek were taken at a downstream lagoon. These data points were excluded from statistical analyses but are included in Supplementary Table S2.

Given the high degree of spatial heterogeneity, differences in landscape geomorphology and hydrology, and the inherently complex watershed response to wildfire, selecting an unburned watershed as a reference site was not possible for this study.

### Sample collection, preparation, and hydrologic monitoring

Samples were collected between October 2020 and May 2021, capturing base, low, and high flow conditions (Supplementary Table S1). Additional watershed flow data were provided by the County of Santa Cruz, United States Geological Survey (USGS), and National Oceanic and Atmospheric Administration (NOAA) National Marine Fisheries Service (Supplementary Information). Water samples were filtered through 0.7- $\mu$ m GF/F filters, which were saved for TSS, POC, and PBC analyses (see Supplementary Information). Aliquots of filtrate were taken for DOC and absorbance analyses. The remaining filtrate was acidified and the dissolved organic matter (DOM) was isolated and recovered via solid-phase extraction (SPE; Dittmar et al. 2008) for DBC analysis (see Supplementary Information).

### Bulk POC, DOC, and absorbance measurements

POC concentrations were determined using an elemental analyzer (see Supplementary Information). DOC concentrations were determined following Stubbins and Dittmar (2012) (see Supplementary Information). Napierian absorbance coefficient at 254 nm ( $a_{254}$ ; Hu et al. 2002) and specific-UV absorbance at 254 nm (SUVA<sub>254</sub>; Weishaar et al. 2003) were determined using absorbance values and DOC concentrations (see Supplementary Information). SUVA<sub>254</sub> and  $a_{254}$  are indicators of DOM aromaticity and chromophoric DOM content, respectively (Weishaar et al. 2003).

### PBC and DBC measurements

Following the benzenepolycarboxylic acid (BPCA) method, condensed aromatic compounds are oxidized to benzenhexacarboxylic acid (B6CA) and benzenepentacarboxylic acid (B5CA), which are subsequently separated and quantified by

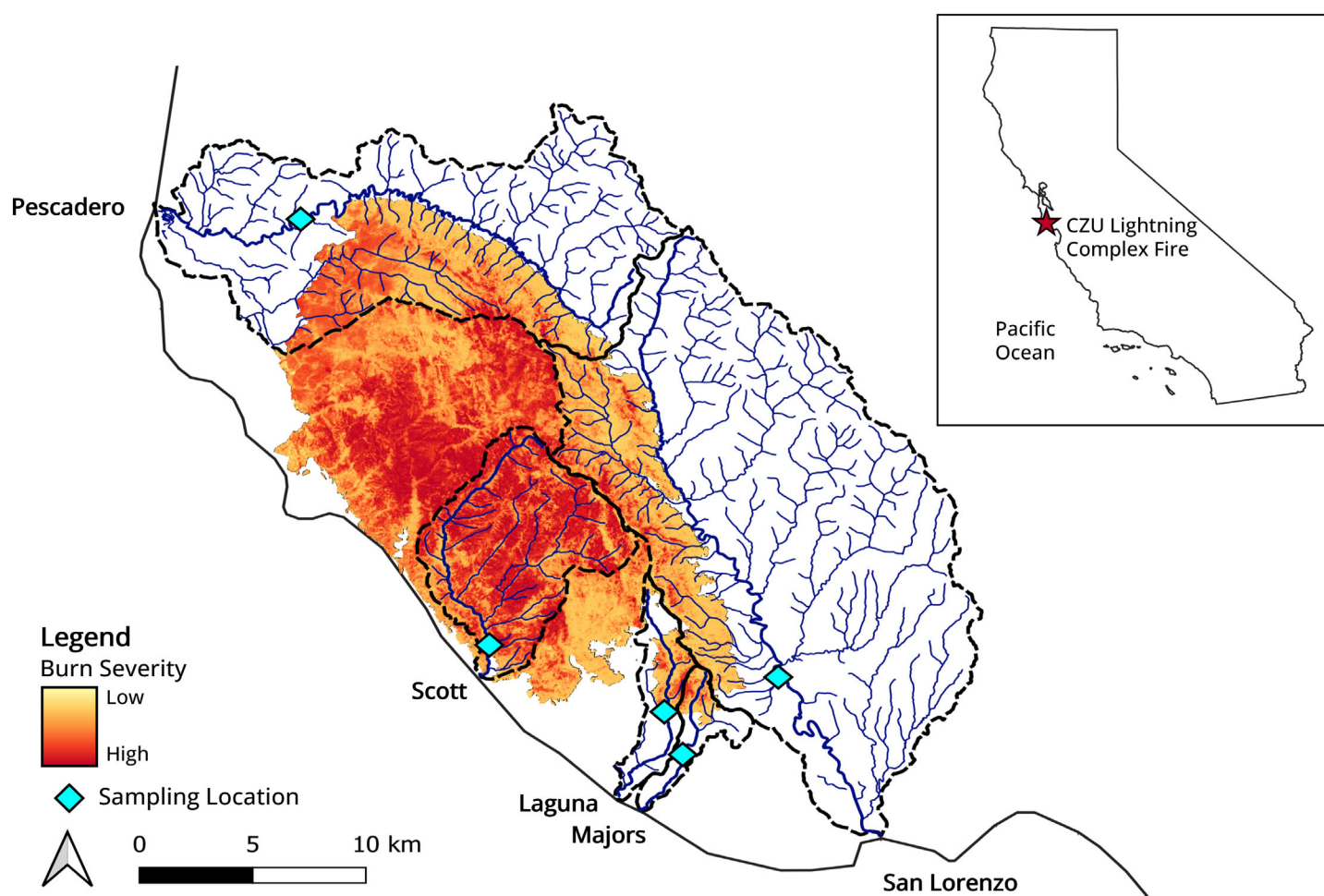


**Fig. 1.** Map of CZU Lightning Complex Fire burn site (California, USA). Sampling locations (blue diamonds) are representative of the five coastal mountain watersheds examined in this study: San Lorenzo River, Pescadero Creek, Majors Creek, Laguna Creek, and Scott Creek. Black dashed lines and solid blue lines are representative of watershed boundaries and streams, respectively. Burn severity of the fire-affected areas is indicated in the legend.

high-performance liquid chromatography (HPLC) (Dittmar 2008; Wagner et al. 2017). BPCA concentrations were used to determine PBC and DBC concentrations in the original sample with an established conversion factor (Stubbins et al. 2015; see Supplemental Information). The ratio of B6CA : B5CA describes the degree of BC polycondensation, where higher ratios indicate a larger and more polycondensed aromatic structure (Glaser et al. 1998; Schneider et al. 2010; Wiedemeier et al. 2015). See Barton and Wagner (2022) for discussion of BPCA conversion factors and a detailed protocol describing BPCA oxidation and DBC quantification by HPLC.

### Statistical analyses

Statistical analyses were conducted using JMP Pro 16. Distributions of data were analyzed for normality via a Shapiro–Wilk test. Differences between groups were assessed with Kruskal–Wallis and specified with Wilcoxon tests. Correlations

were evaluated via Spearman’s rank correlation. Linear relationships with normally distributed residuals were analyzed via simple linear regression. To facilitate statistical comparisons, quantitative and qualitative measurements were binned by flow category (baseflow, low flow, high flow; Supplementary Table S1). See Tables 1, S2, and S3 for data and details of statistical analyses.

## Results

### Effect of burn extent on material export

Mean values of POC, DOC, DBC, and DBC : DOC did not vary significantly among watersheds of variable burn extent ( $p > 0.05$ ; Table 1; Supplementary Table S3). Although mean PBC and PBC : POC ratios varied across burn extents ( $p < 0.05$ ; Table 1; Supplementary Table S3), there was no significant difference between values from watersheds with the highest (98%; Scott Creek) and lowest (20%; San Lorenzo



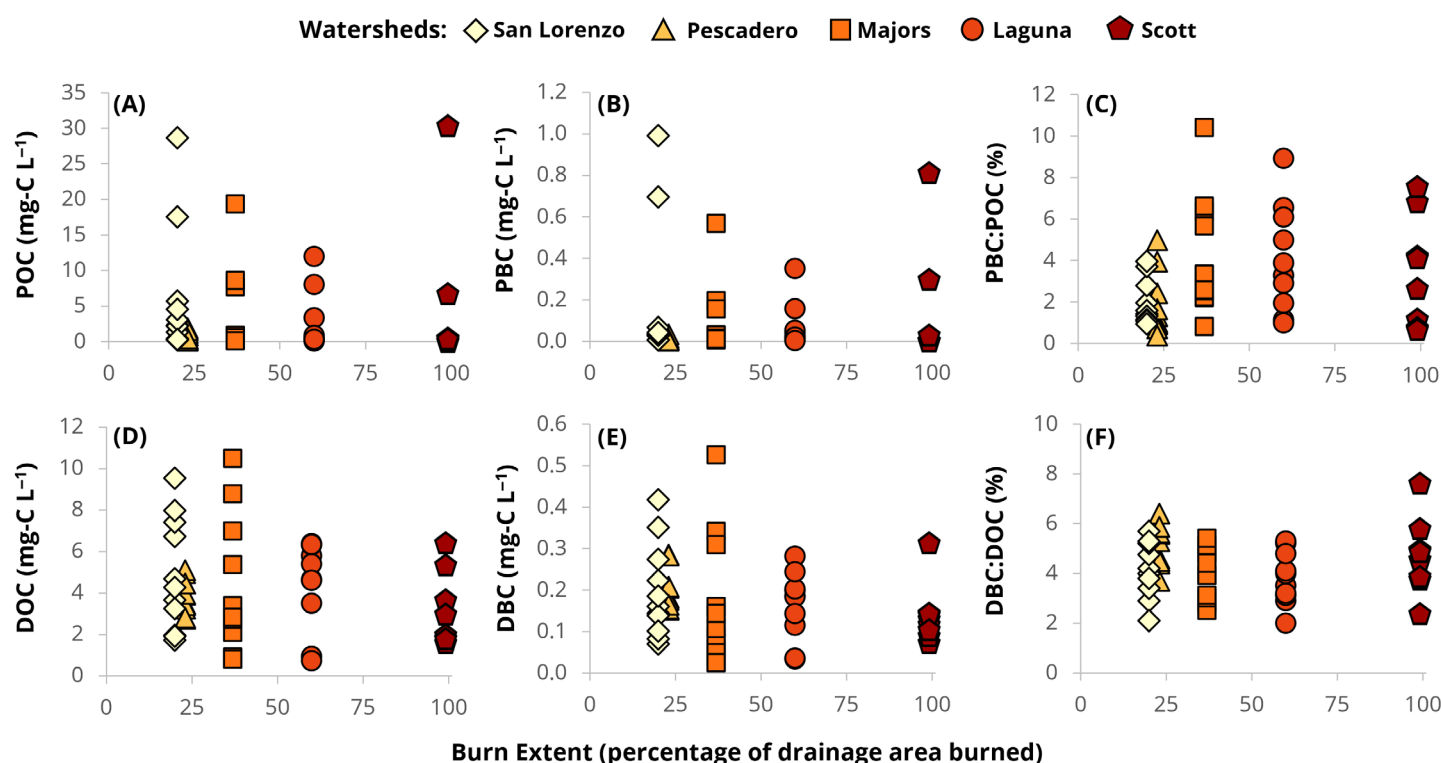


**Fig. 2.** Relationships between watershed burn extent and (A) POC concentrations, (B) PBC concentrations, and (C) the ratio of PBC to POC (PBC : POC), (D) DOC concentrations, (E) DBC concentrations, and (F) the ratio of DBC to DOC (DBC : DOC).

River) burn extents ( $p > 0.05$ ). Only the PBC : POC and PBC : TSS ratios (among carbon concentrations and ratios; Fig. 2; Supplementary Fig. S2) were found to have a significant correlation to burn extent ( $p < 0.05$ ; Fig. 2C). None of the other variables (TSS,  $a_{254}$ ,  $SUVA_{254}$ , and B6CA : B5CA ratios) showed a significant correlation with burn extent ( $p > 0.05$ ; Supplementary Fig. S2; Table S3).

Like burn extent, only PBC : POC had a significant correlation with catchment size ( $p < 0.05$ ; Supplementary Table S3). The relationship between catchment slope and OC and BC concentrations was negative due to the watershed with the largest slope having the least exported particulate material ( $p < 0.05$ ; Supplementary Table S3; see Supplementary Information for more information).

#### Variable coupling between OC and BC export

Overall, DBC was linearly related with DOC (slope = 0.038;  $R^2 = 0.74$ ;  $p < 0.0001$ ; Fig. 3F), though we observed temporal variability in the slope and strength of these relationships for each catchment (Fig. 3A–E). This linear relationship was more positive and stronger in 2021 (January to May; slope = 0.045;  $R^2 = 0.90$ ;  $p < 0.0001$ ; Fig. 3F) than in 2020 (October to December; slope = 0.025;  $R^2 = 0.75$ ;  $p < 0.0001$ ; Fig. 3F). DBC and DBC : DOC values were greater in 2021 than in 2020 ( $p < 0.05$ ) whereas DOC concentrations were not significantly

different between years ( $p > 0.05$ ). Since the time of fire, the ratio of DBC : DOC increased with successive sampling dates ( $p < 0.0001$ ; Supplementary Fig. S3). Similarly, PBC was positively correlated with both POC and TSS ( $p < 0.0001$ ; Supplementary Fig. S6; Table S3) with a more positive correlation from January to May 2021 than from October to December 2020 ( $p < 0.05$ ; Supplementary Fig. S6F; Table S3).

#### Effect of hydrology on material export

The geographic proximity of the five coastal watersheds resulted in similar temporal responses to hydrologic events, but their differences in basin size and watershed characteristics were reflected in discharge magnitudes varying among individual catchments (Fig. 4A). With data from all watersheds combined, mean POC, PBC, DOC, DBC, TSS, and  $a_{254}$  values increased consecutively from baseflow to high flow ( $p < 0.01$ ; Supplementary Fig. S5). Ratios of PBC : POC and B6CA : B5CA (for PBC) did not vary significantly between flow categories ( $p > 0.1$ ) whereas B6CA : B5CA ratios (for DBC) were significantly different only between high flow and other flows ( $p < 0.05$ ). Mean PBC : TSS, values decreased with increased flow ( $p < 0.01$ ). DBC : DOC and  $SUVA_{254}$  values were only significantly different between low flow and other flows ( $p < 0.5$ ). See Supplemental Information for watershed-specific trends with flow category.

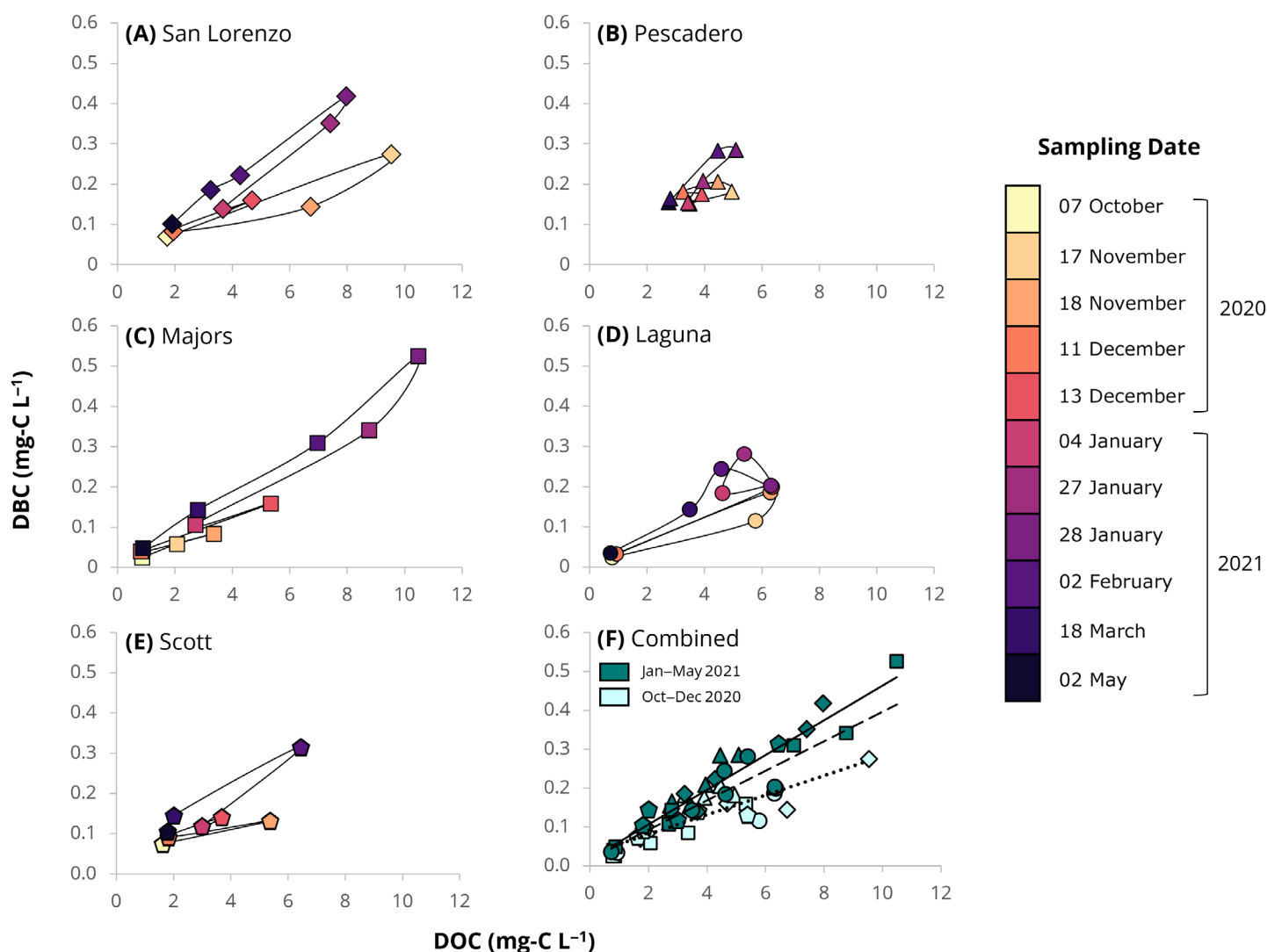


**Fig. 3.** DBC vs. DOC for individual watersheds: (A) San Lorenzo ( $n = 11$ , diamond symbols), (B) Pescadero ( $n = 11$ , triangle symbols), (C) Majors ( $n = 11$ , square symbols), (D) Laguna ( $n = 11$ , circle symbols), (E) Scott ( $n = 8$ , pentagon symbols), and (F) all samples combined ( $n = 52$ ). Linear relationships between DBC and DOC concentrations shown in (F) were determined for: all samples combined (dashed line; slope = 0.038;  $R^2 = 0.74$ ;  $p < 0.0001$ ), samples taken in October 2020 to December 2020 (dotted line; slope = 0.025;  $R^2 = 0.75$ ;  $p < 0.0001$ ), and samples taken from January 2021 to May 2021 (solid line; slope = 0.045;  $R^2 = 0.90$ ;  $p < 0.0001$ ). Note that no sample was collected from Scott Creek on 17 November 2020, and those collected on 27 January 2021 and 28 January 2021 are not included here (see “Methods” section). The connection between points in (A–E) are to help visualize the temporal sequence of sample results.

Values of POC, PBC, DOC, DBC, TSS, PBC : TSS, and  $a_{254}$  were significantly and positively correlated with discharge ( $p < 0.05$ ; Supplementary Table S3). PBC : POC, DBC : DOC,  $SUVA_{254}$ , and B6CA : B5CA ratios were not significantly correlated with discharge ( $p > 0.05$ ; Supplementary Table S3). Flow-dependent coupling of particulate and dissolved phases was also observed overall, but when examined by flow category, phases were coupled only at high flow ( $p < 0.05$ ; Supplementary Fig. S4; Table S3), see Supplementary Information for further details.

## Discussion

### Hydrology, rather than burn extent, drives OC and BC export post-fire

The interaction of burned landscapes with water, especially in the 1<sup>st</sup> year post-fire, determines the fate of pyrogenic carbon (Masiello and Berhe 2020). PBC and POC require dry-ravel or erosional processes to move from landscape to stream channel, and can be mobilized through re-suspension mechanisms from intermediate deposits (Bird et al. 2015; Coppola et al. 2018). In other Western US watersheds,

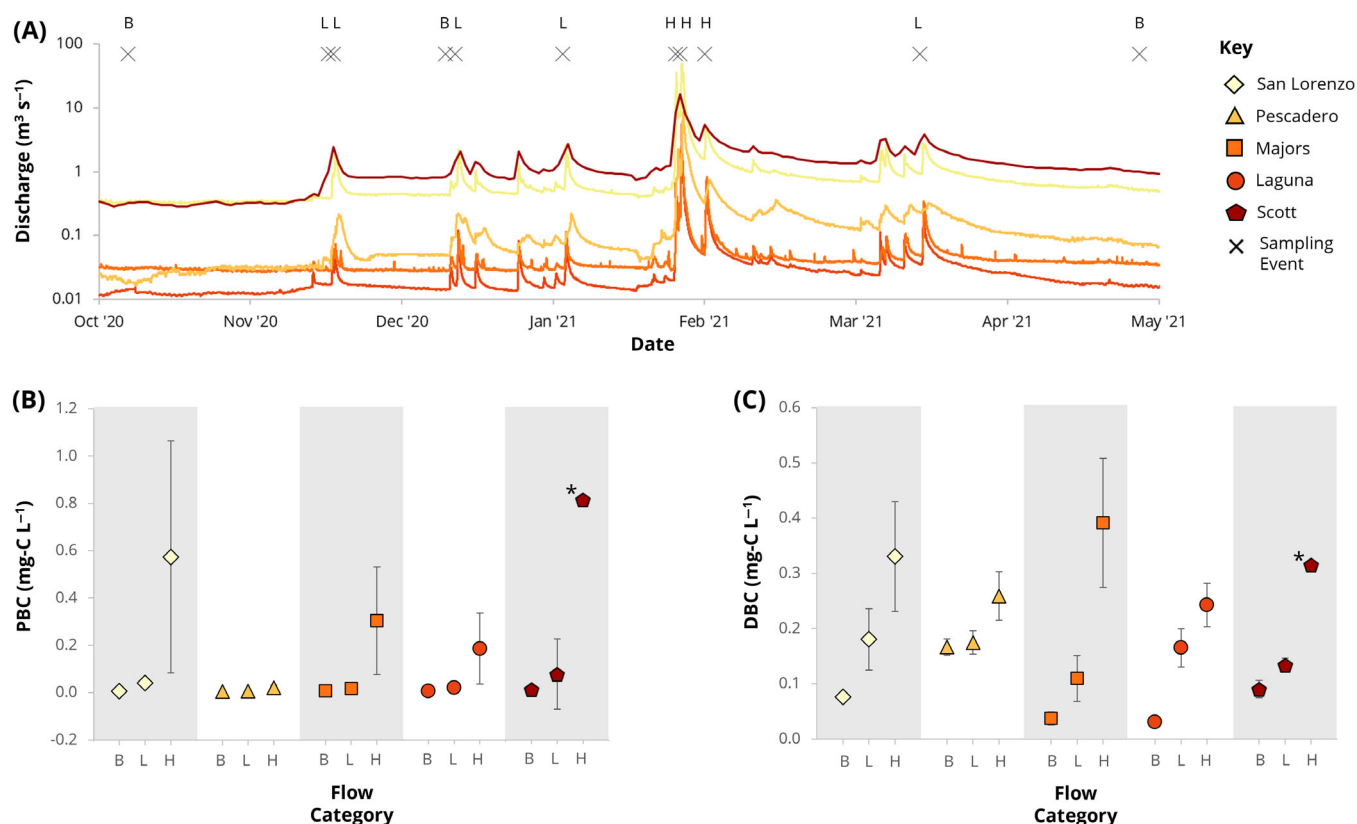


**Fig. 4.** (A) Stream discharge over the study period (specify). Sampling events, which are indicated by crosses along the x-axis in (A), were differentiated by flow category: baseflow (B), low flow (L), and high flow (H). (B, C) Average PBC and DBC concentrations at baseflow, low flow, and high flow for the San Lorenzo River (light yellow diamond), Pescadero Creek (yellow triangle), Majors Creek (orange square), Laguna Creek (red circle), and Scott Creek (dark red pentagon). Symbols indicate average values, and error bars represent standard deviations. The asterisk (\*) signifies that there was only one sample therefore there are no standard deviations displayed.

increased TSS and pyrogenic carbon concentrations have been related to fire activity (Burke et al. 2013; Wagner et al. 2015; Rust et al. 2018; Barron et al. 2022). In our comparisons across watersheds, we observed no relation between burn extent and the absolute magnitude of TSS, POC, and PBC. However, the concentrations of particulate materials did increase with increased water discharge. It should be noted that the variability in watershed area and average catchment slope, combined with a lack of pre-fire data, may have masked some of the burn impacts on carbon export.

Unlike POC and PBC, DOC and DBC export from landscape to stream channel is restricted by solubility, which is probably why the latter are often inconsistently or indirectly correlated to wildfire activity (Ding et al. 2013; Wagner et al. 2015; Raelison et al. 2023). Our results support this explanation, as DBC and DOC concentrations were not related to burn extent (Fig. 2). However, increases in water discharge have been related to increases in DOC and DBC export (Raymond and Sifers 2010; Dhillon and Inamdar 2014; Wagner et al. 2015; Roebuck et al. 2018, 2022). There is also evidence that storm events can enhance the amounts of

wildfire-generated chromophoric DOM exported during storm events (Roebuck et al. 2022). We also observed that increased discharge resulted in the export of greater amounts of bulk DOC, DBC, and chromophoric DOM (Supplementary Fig. S5; Table S3).

Burn extent, while easy to determine, is not always a useful predictor of post-fire OC or BC export as it lacks watershed- and fire-specific nuance that can be more determinant of organic matter export (e.g., rainfall, runoff, slope, burn severity, vegetation, lithology; Connolly et al. 2018; Santos et al. 2019; Williamson et al. 2021; Clark et al. 2022). PBC : POC and PBC : TSS were the only parameters with a significant correlation with burn extent in our study (Fig. 2; Supplementary Fig. S1). This leads us to conclude that percentage of watershed area burned is not a primary control on the absolute magnitude of BC or OC concentrations within the 1<sup>st</sup> year post-fire in California coastal mountain watersheds affected by the CZU Lightning Complex Fires.

Although coastal rivers have been identified as major contributors of BC to coastal waters (Nakane et al. 2017), riverine fluxes of BC and OC to coastal waters remain

relatively unconstrained. Here, back-of-the-envelope calculations reveal these five small mountain rivers combined would export an estimated  $100,000 \pm 1000$  kg-POC,  $71000 \pm 600$  kg-DOC,  $430 \pm 1000$  kg-PBC, and  $3500 \pm 700$  kg-DBC annually if storm events are excluded. Just one day at high flow would result in a 6- and five-fold increase in annual fluxes of POC and PBC, respectively. Similarly, annual fluxes of DOC and DBC would increase by 27% (see Supplementary Information). Our observations of increased OC and BC concentrations with increased flow (Fig. 4; Supplementary Fig. S3), point to hydrology as the main mechanism for transferring material from landscape to stream after a wildfire occurs, wherein stream flow rather than solute concentrations drive material export. Further work, particularly in systems with pre-fire data, may elucidate additional drivers of organic matter export post-fire, highlight common responses in fire-affected systems, and improve our understanding of variability in post-fire export.

### Relationships between DBC and DOC vary temporally in fire-affected coastal mountain rivers

The proportion of DBC to DOC ranges from 0.1% to 18% among river systems globally (Jaffé et al. 2013; Jones et al. 2020). Here, DBC : DOC was  $4.3\% \pm 1.2\%$  on average, which is similar to what has been observed for other temperate rivers (Jones et al. 2020). The strength of the DBC vs. DOC relationship among all rivers evaluated in this study ( $R^2 = 0.74$ ;  $p < 0.0001$ ) was lower than the global relationship established by Jaffé et al. (2013). The degree of scatter we observed in this relationship likely results from our higher sampling frequency, which captured temporal and within-storm variability of carbon export in each catchment. Small mountain rivers have shorter water residence times than global rivers, thus in-stream DOM experiences overall less biogeochemical processing and reflects source-specific DOM signatures.

The slope of the DBC vs. DOC relationship was lower in October 2020 to December 2020 than in January 2021 to May 2021 (Fig. 3). With data from all watersheds combined, concentrations of DOC were not significantly different during the 2020 and 2021 sampling periods ( $p > 0.05$ ), but DBC and DBC : DOC were significantly greater in 2021 ( $p < 0.05$ ). Given that there was no significant difference in DBC : DOC ratio between baseflow and high flow, we suggest that the solubility restrictions around DBC export, not hydrology alone, play a role in the increase in DBC : DOC ratios over time (Supplementary Fig. S3). Due to its condensed aromatic structure, particulate charcoal (i.e., PBC) is buoyant and hydrophobic; its molecular structure must be altered by degradation and oxidation before it can enter aquatic systems in the dissolved phase (Abiven et al. 2011; Brewer et al. 2014). PBC has been found to leach substantial amounts of DBC (Abiven et al. 2011; Roebuck et al. 2017; Wagner et al. 2021). Furthermore, the aging of BC in soils results in the addition of polar functional groups, thus, enhancing its solubility in

water (Cheng et al. 2008; Wozniak et al. 2020). As the 2021 sampling events coincided with the largest storm events, the preferential increase in DBC concentrations relative to DOC may be due to increased discharge. It is also possible that subsequent wetting events played a role in the oxidation and preferential export of DBC relative to DOC (Nguyen and Lehmann 2009).

### Evaluation of potential predictor variables for post-fire BC export

We found TSS and POC to be significantly correlated to PBC concentrations; a coupling which has also been established in other systems (Wagner et al. 2015; Xu et al. 2016; Coppola et al. 2018; Supplementary Fig. S5). Our data show a strong relationship between DBC and both DOC (Fig. 3F) and  $a_{254}$  ( $[DBC] = 0.0062 \times a_{254}$ ,  $R^2 = 0.86$ ,  $p < 0.0001$ ; Supplementary Fig. S8), which have also been established in a variety of systems (Jaffé et al. 2013; Stubbins et al. 2015; Wagner et al. 2019). In brief, we suggest that TSS and POC may be used to estimate PBC concentrations, and  $a_{254}$  and DOC may be used to estimate DBC concentrations. However, given the inter-watershed variability, we suggest that these relationships be evaluated and established regionally.

### Conclusions

Our study indicates that OC export from fire-affected small mountain rivers to the ocean in the 1<sup>st</sup> year post-fire is primarily driven by hydrology rather than by burn extent. This is because OC and BC concentrations increased during event flows yet varied little despite a large disparity in the percentage of individual watershed burned (20–98%). Our results also highlight the potential impact of post-fire storms on material export to coastal systems—one event at high flow alone could result in a 500%, 400%, 27%, and 27% increase in annual export of POC, PBC, DOC, and DBC, respectively. While the actual fate of organic matter was not examined here, this material could be deposited in secondary reservoirs, be sequestered in oceanic sediments or remain dissolved in the water column to photodegrade and/or be utilized by coastal microbes (Stubbins et al. 2012; Coppola et al. 2014; Nakane et al. 2017). Although questions remain about the watershed-specific controls of post-fire organic matter export, water discharge has been identified as a major variable and must be considered in future export models.

### References

- Abiven, S., P. Hengartner, M. P. W. Schneider, N. Singh, and M. W. I. Schmidt. 2011. Pyrogenic carbon soluble fraction is larger and more aromatic in aged charcoal than in fresh charcoal. *Soil Biol. Biochem.* **43**: 1615–1617. doi:10.1016/j.soilbio.2011.03.027
- Abney, R. B., T. J. Kuhn, A. Chow, W. Hockaday, M. L. Fogel, and A. A. Berhe. 2019. Pyrogenic carbon erosion after the



- Rim Fire, Yosemite National Park: The Role of Burn Severity and Slope. *J. Geophys. Res. Biogeo.* **124**: 432–449. doi:[10.1029/2018JG004787](https://doi.org/10.1029/2018JG004787)
- Barron, S. M., N. Mladenov, K. E. Sant, and A. M. Kinoshita. 2022. Surface water quality after the Woolsey fire in Southern California. *Water Air Soil Pollut.* **233**: 1–20. doi:[10.1007/s11270-022-05844-x](https://doi.org/10.1007/s11270-022-05844-x)
- Barton, R., and S. Wagner. 2022. Measuring dissolved black carbon in water via aqueous, inorganic, high-performance liquid chromatography of benzenepolycarboxylic acid (BPCA) molecular markers. *PLoS One* **15**: 1–8. doi:[10.1371/journal.pone.0268059](https://doi.org/10.1371/journal.pone.0268059)
- Bird, M. I., J. G. Wynn, G. Saiz, C. M. Wurster, and A. McBeath. 2015. The pyrogenic carbon cycle. *Annu. Rev. Earth Planet. Sci.* **43**: 273–298. doi:[10.1146/annurev-earth-060614-105038](https://doi.org/10.1146/annurev-earth-060614-105038)
- Bond, T. C., and others. 2013. Bounding the role of black carbon in the climate system: A scientific assessment. *J. Geophys. Res. Atmos.* **118**: 5380–5552. doi:[10.1002/jgrd.50171](https://doi.org/10.1002/jgrd.50171)
- Bowman, D. M. J. S., C. A. Kolden, J. T. Abatzoglou, F. H. Johnston, G. R. van der Werf, and M. Flannigan. 2020. Vegetation fires in the Anthropocene. *Nat. Rev. Earth Environ.* **1**: 500–515. doi:[10.1038/s43017-020-0085-3](https://doi.org/10.1038/s43017-020-0085-3)
- Brewer, C. E., and others. 2014. New approaches to measuring biochar density and porosity. *Biomass Bioenergy* **66**: 176–185. doi:[10.1016/j.biombioe.2014.03.059](https://doi.org/10.1016/j.biombioe.2014.03.059)
- Burke, M. P., T. S. Hogue, A. M. Kinoshita, J. Barco, C. Wessel, and E. D. Stein. 2013. Pre- and post-fire pollutant loads in an urban fringe watershed in Southern California. *Environ. Monit. Assess.* **185**: 10131–10145. doi:[10.1007/s10661-013-3318-9](https://doi.org/10.1007/s10661-013-3318-9)
- Cawley, K. M., A. K. Hohner, D. C. Podgorski, W. T. Cooper, J. A. Korak, and F. L. Rosario-Ortiz. 2017. Molecular and spectroscopic characterization of water extractable organic matter from thermally altered soils reveal insight into disinfection byproduct precursors. *Environ. Sci. Technol.* **51**: 771–779. doi:[10.1021/acs.est.6b05126](https://doi.org/10.1021/acs.est.6b05126)
- Chen, H., J. Wang, X. Zhao, Y. Wang, Z. Huang, T. Gong, and Q. Xian. 2022. Occurrence of dissolved black carbon in source water and disinfection byproducts formation during chlorination. *J. Hazard. Mater.* **435**: 129054. doi:[10.1016/j.jhazmat.2022.129054](https://doi.org/10.1016/j.jhazmat.2022.129054)
- Cheng, C. H., J. Lehmann, and M. H. Engelhard. 2008. Natural oxidation of black carbon in soils: Changes in molecular form and surface charge along a climosequence. *Geochim. Cosmochim. Acta* **72**: 1598–1610. doi:[10.1016/j.gca.2008.01.010](https://doi.org/10.1016/j.gca.2008.01.010)
- Clark, K. E., R. F. Stallard, S. F. Murphy, M. A. Scholl, G. González, A. F. Plante, and W. H. McDowell. 2022. Extreme rainstorms drive exceptional organic carbon export from forested humid-tropical rivers in Puerto Rico. *Nat. Commun.* **13**: 1–8. doi:[10.1038/s41467-022-29618-5](https://doi.org/10.1038/s41467-022-29618-5)
- Connolly, C. T., M. S. Khosh, G. A. Burkart, T. A. Douglas, R. M. Holmes, A. D. Jacobson, S. E. Tank, and J. W. McClelland. 2018. Watershed slope as a predictor of fluvial dissolved organic matter and nitrate concentrations across geographical space and catchment size in the Arctic. *Environ. Res. Lett.* **13**: 1–9. doi:[10.1088/1748-9326/aac35d](https://doi.org/10.1088/1748-9326/aac35d)
- Coppola, A. I., L. A. Ziolkowski, C. A. Masiello, and E. R. M. Druffel. 2014. Aged black carbon in marine sediments and sinking particles. *Geophys. Prospect.* **41**: 2427–2433. doi:[10.1002/2013GL059068](https://doi.org/10.1002/2013GL059068)
- Coppola, A. I., and others. 2018. Global-scale evidence for the refractory nature of riverine black carbon. *Nat. Geosci.* **11**: 584–588. doi:[10.1038/s41561-018-0159-8](https://doi.org/10.1038/s41561-018-0159-8)
- Coppola, A. I., S. Wagner, S. T. Lennartz, M. Seidel, N. D. Ward, T. Dittmar, C. Santín, and M. W. Jones. 2022. The black carbon cycle and its role in the Earth system. *Nat. Rev. Earth Environ.* **3**: 516–532. doi:[10.1038/s43017-022-00316-6](https://doi.org/10.1038/s43017-022-00316-6)
- Cotrufo, M. F., and others. 2016. Redistribution of pyrogenic carbon from hillslopes to stream corridors following a large montane wildfire. *Global Biogeochem. Cycl.* **30**: 1348–1355. doi:[10.1002/2016GB005467](https://doi.org/10.1002/2016GB005467)
- Dhillon, G. S., and S. Inamdar. 2014. Storm event patterns of particulate organic carbon (POC) for large storms and differences with dissolved organic carbon (DOC). *Biogeochemistry* **118**: 61–81. doi:[10.1007/s10533-013-9905-6](https://doi.org/10.1007/s10533-013-9905-6)
- Ding, Y., Y. Yamashita, W. K. Dodds, and R. Jaffé. 2013. Dissolved black carbon in grassland streams: Is there an effect of recent fire history? *Chemosphere* **90**: 2557–2562. doi:[10.1016/j.chemosphere.2012.10.098](https://doi.org/10.1016/j.chemosphere.2012.10.098)
- Dittmar, T. 2008. The molecular level determination of black carbon in marine dissolved organic matter. *Org. Geochem.* **39**: 396–407. doi:[10.1016/j.orggeochem.2008.01.015](https://doi.org/10.1016/j.orggeochem.2008.01.015)
- Dittmar, T., B. Koch, N. Hertkorn, and G. Kattner. 2008. A simple and efficient method for the solid-phase extraction of dissolved organic matter (SPE-DOM) from seawater. *Limnol. Oceanogr. Methods* **6**: 230–235. doi:[10.4319/lom.2008.6.230](https://doi.org/10.4319/lom.2008.6.230)
- Ellis, T. M., D. M. J. S. Bowman, P. Jain, M. D. Flannigan, and G. J. Williamson. 2022. Global increase in wildfire risk due to climate-driven declines in fuel moisture. *Glob. Chang. Biol.* **28**: 1544–1559. doi:[10.1111/gcb.16006](https://doi.org/10.1111/gcb.16006)
- Galy, V., B. Peucker-Ehrenbrink, and T. Eglinton. 2015. Global carbon export from the terrestrial biosphere controlled by erosion. *Nature* **521**: 204–207. doi:[10.1038/nature14400](https://doi.org/10.1038/nature14400)
- Glaser, B., L. Haumaier, G. Guggenberger, and W. Zech. 1998. Black carbon in soils: The use of benzenecarboxylic acids as specific markers. *Org. Geochem.* **29**: 811–819. doi:[10.1016/S0146-6380\(98\)00194-6](https://doi.org/10.1016/S0146-6380(98)00194-6)
- Goldberg, E. D. 1985. *Black carbon in the environment: Properties and distribution*. Wiley, New York.
- Gorancov, A. I., M. F. Schaller, J. A. Long, D. C. Podgorski, and S. Wagner. 2021. Characterization of asphaltene and petroleum using benzenepolycarboxylic acids (BPCAs) and compound-specific stable carbon isotopes. *Energy Fuels* **35**: 18135–18145. doi:[10.1021/acs.energyfuels.1c02374](https://doi.org/10.1021/acs.energyfuels.1c02374)

- Hohner, A. K., C. C. Rhoades, P. Wilkerson, and F. L. Rosario-Ortiz. 2019. Wildfires alter forest watersheds and threaten drinking water quality. *Acc. Chem. Res.* **52**: 1234–1244. doi:[10.1021/acs.accounts.8b00670](https://doi.org/10.1021/acs.accounts.8b00670)
- Hu, C., F. E. Muller-Karger, and R. G. Zepp. 2002. Absorbance, absorption coefficient, and apparent quantum yield: A comment on common ambiguity in the use of these optical concepts. *Limnol. Oceanogr.* **47**: 1261–1267. doi:[10.4319/lo.2002.47.4.1261](https://doi.org/10.4319/lo.2002.47.4.1261)
- Hunsinger, G. B., S. Mitra, J. A. Warrick, and C. R. Alexander. 2008. Oceanic loading of wildfire-derived organic compounds from a small mountainous river. *J. Geophys. Res.* **113**: 1–14. doi:[10.1029/2007JG000476](https://doi.org/10.1029/2007JG000476)
- Jaffé, R., Y. Ding, J. Niggemann, A. V. Vähätalo, A. Stubbins, R. G. M. Spencer, J. Campbell, and T. Dittmar. 2013. Global charcoal mobilization from soils via dissolution and riverine transport to the oceans. *Science* **340**: 345–347. doi:[10.1126/science.1231476](https://doi.org/10.1126/science.1231476)
- Jensen, A. M., T. M. Scanlon, and A. L. Riscassi. 2017. Emerging investigator series: The effect of wildfire on streamwater mercury and organic carbon in a forested watershed in the southeastern United States. *Environ Sci Process Impacts* **19**: 1505–1517. doi:[10.1039/c7em00419b](https://doi.org/10.1039/c7em00419b)
- Jones, M. W., C. Santín, G. R. van der Werf, and S. H. Doerr. 2019. Global fire emissions buffered by the production of pyrogenic carbon. *Nat. Geosci.* **12**: 742–747. doi:[10.1038/s41561-019-0403-x](https://doi.org/10.1038/s41561-019-0403-x)
- Jones, M. W., A. I. Coppola, C. Santín, T. Dittmar, R. Jaffé, S. H. Doerr, and T. A. Quine. 2020. Fires prime terrestrial organic carbon for riverine export to the global oceans. *Nat. Commun.* **11**: 4–11. doi:[10.1038/s41467-020-16576-z](https://doi.org/10.1038/s41467-020-16576-z)
- Kuzyakov, Y., I. Bogomolova, and B. Glaser. 2014. Biochar stability in soil: Decomposition during eight years and transformation as assessed by compound-specific  $^{14}\text{C}$  analysis. *Soil Biol. Biochem.* **70**: 229–236. doi:[10.1016/j.soilbio.2013.12.021](https://doi.org/10.1016/j.soilbio.2013.12.021)
- Masiello, C. A. 2004. New directions in black carbon organic geochemistry. *Mar. Chem.* **92**: 201–213. doi:[10.1016/j.marchem.2004.06.043](https://doi.org/10.1016/j.marchem.2004.06.043)
- Masiello, C. A., and E. R. M. Druffel. 2001. Carbon isotope geochemistry of the Santa Clara River. *Global Biogeochem. Cycl.* **15**: 407–416. doi:[10.1029/2000GB001290](https://doi.org/10.1029/2000GB001290)
- Masiello, C. A., and A. A. Berhe. 2020. First interactions with the hydrologic cycle determine pyrogenic carbon's fate in the Earth system. *Earth Surf. Process. Landforms* **45**: 2394–2398. doi:[10.1002/esp.4925](https://doi.org/10.1002/esp.4925)
- Nakane, M., T. Ajioka, and Y. Yamashita. 2017. Distribution and sources of dissolved black carbon in surface waters of the Chukchi Sea, Bering Sea, and the North Pacific Ocean. *Front. Earth Sci.* **5**: 1–12. doi:[10.3389/feart.2017.00034](https://doi.org/10.3389/feart.2017.00034)
- Nguyen, B. T., and J. Lehmann. 2009. Black carbon decomposition under varying water regimes. *Org. Geochem.* **40**: 846–853. doi:[10.1016/j.orggeochem.2009.05.004](https://doi.org/10.1016/j.orggeochem.2009.05.004)
- Nunes, J. P., and others. 2018. Assessing water contamination risk from vegetation fires: Challenges, opportunities and a framework for progress. *Hydrol. Process.* **32**: 687–694. doi:[10.1002/hyp.11434](https://doi.org/10.1002/hyp.11434)
- Podgorski, D. C., and others. 2021. Hydrocarbons to carboxyl-rich alicyclic molecules: A continuum model to describe biodegradation of petroleum-derived dissolved organic matter in contaminated groundwater plumes. *J. Hazard. Mater.* **402**: 123998. doi:[10.1016/j.jhazmat.2020.123998](https://doi.org/10.1016/j.jhazmat.2020.123998)
- Raelison, O. D., R. Valenca, A. Lee, S. Karim, J. P. Webster, B. A. Poulin, and S. K. Mohanty. 2023. Wildfire impacts on surface water quality parameters: Cause of data variability and reporting needs. *Environ. Pollut.* **317**: 120713. doi:[10.1016/j.envpol.2022.120713](https://doi.org/10.1016/j.envpol.2022.120713)
- Raymond, P. A., and J. E. Saiers. 2010. Event controlled DOC export from forested watersheds. *Biogeochemistry* **100**: 197–209. doi:[10.1007/s10533-010-9416-7](https://doi.org/10.1007/s10533-010-9416-7)
- Robinne, F. N., K. D. Bladon, C. Miller, M. A. Parisien, J. Mathieu, and M. D. Flannigan. 2018. A spatial evaluation of global wildfire-water risks to human and natural systems. *Sci. Total Environ.* **610–611**: 1193–1206. doi:[10.1016/j.scitotenv.2017.08.112](https://doi.org/10.1016/j.scitotenv.2017.08.112)
- Robinne, F. N., and others. 2021. Scientists' warning on extreme wildfire risks to water supply. *Hydrol. Process.* **35**: 1–11. doi:[10.1002/hyp.14086](https://doi.org/10.1002/hyp.14086)
- Roebuck, J. A., D. C. Podgorski, S. Wagner, and R. Jaffé. 2017. Photodissolution of charcoal and fire-impacted soil as a potential source of dissolved black carbon in aquatic environments. *Org. Geochem.* **112**: 16–21. doi:[10.1016/j.orggeochem.2017.06.018](https://doi.org/10.1016/j.orggeochem.2017.06.018)
- Roebuck, J. A., P. M. Medeiros, M. L. Letourneau, and R. Jaffé. 2018. Hydrological controls on the seasonal variability of dissolved and particulate black carbon in the Altamaha River, GA. *J. Geophys. Res. Biogeosci.* **123**: 3055–3071. doi:[10.1029/2018JG004406](https://doi.org/10.1029/2018JG004406)
- Roebuck, J. A. J., and others. 2022. Spatiotemporal controls on the delivery of dissolved organic matter to streams following a wildfire. *Geophys. Res. Lett.* **49**: 1–11. doi:[10.1029/2022GL099535](https://doi.org/10.1029/2022GL099535)
- Rust, A. J., T. S. Hogue, S. Saxe, and J. McCray. 2018. Post-fire water-quality response in the western United States. *Int. J. Wildland Fire* **27**: 203–216. doi:[10.1071/WF17115](https://doi.org/10.1071/WF17115)
- Santos, F., A. S. Wymore, B. K. Jackson, S. M. P. Sullivan, W. H. McDowell, and A. A. Berhe. 2019. Fire severity, time since fire, and site-level characteristics influence streamwater chemistry at baseflow conditions in catchments of the Sierra Nevada, California, USA. *Fire Ecol.* **15**: 1–15. doi:[10.1186/s42408-018-0022-8](https://doi.org/10.1186/s42408-018-0022-8)
- Schneider, M. P. W., M. Hilf, U. F. Vogt, and M. W. I. Schmidt. 2010. The benzene polycarboxylic acid (BPCA) pattern of wood pyrolyzed between 200°C and 1000°C. *Org. Geochem.* **41**: 1082–1088. doi:[10.1016/j.orggeochem.2010.07.001](https://doi.org/10.1016/j.orggeochem.2010.07.001)

- Shakesby, R. A., S. H. Doerr, and R. P. D. Walsh. 2000. The erosional impact of soil hydrophobicity: Current problems and future research directions. *J. Hydrol.* **231–232**: 178–191. doi:[10.1016/S0022-1694\(00\)00193-1](https://doi.org/10.1016/S0022-1694(00)00193-1)
- Shakesby, R. A., and S. H. Doerr. 2006. Wildfire as a hydrological and geomorphological agent. *Earth Sci. Rev.* **74**: 269–307. doi:[10.1016/j.earscirev.2005.10.006](https://doi.org/10.1016/j.earscirev.2005.10.006)
- Shakesby, R. A., J. A. Moody, D. A. Martin, and P. R. Robichaud. 2016. Synthesizing empirical results to improve predictions of post-wildfire runoff and erosion responses. *Int. J. Wildland Fire* **25**: 257–261. doi:[10.1071/WF16021](https://doi.org/10.1071/WF16021)
- Stubbins, A., and T. Dittmar. 2012. Low volume quantification of dissolved organic carbon and dissolved nitrogen. *Limnol. Oceanogr. Methods* **10**: 347–352. doi:[10.4319/lom.2012.10.347](https://doi.org/10.4319/lom.2012.10.347)
- Stubbins, A., J. Niggemann, and T. Dittmar. 2012. Photolability of deep ocean dissolved black carbon. *Biogeosciences* **9**: 1661–1670. doi:[10.5194/bg-9-1661-2012](https://doi.org/10.5194/bg-9-1661-2012)
- Stubbins, A., R. G. M. Spencer, P. J. Mann, R. M. Holmes, J. W. McClelland, J. Niggemann, and T. Dittmar. 2015. Utilizing colored dissolved organic matter to derive dissolved black carbon export by arctic rivers. *Front. Earth Sci.* **3**: 1–11. doi:[10.3389/feart.2015.00063](https://doi.org/10.3389/feart.2015.00063)
- Uzun, H., R. A. Dahlgren, C. Olivares, C. U. Erdem, T. Karanfil, and A. T. Chow. 2020. Two years of post-wildfire impacts on dissolved organic matter, nitrogen, and precursors of disinfection by-products in California stream waters. *Water Res.* **181**: 115891. doi:[10.1016/j.watres.2020.115891](https://doi.org/10.1016/j.watres.2020.115891)
- Wagner, S., K. M. Cawley, F. L. Rosario-Ortiz, and R. Jaffé. 2015. In-stream sources and links between particulate and dissolved black carbon following a wildfire. *Biogeochemistry* **124**: 145–161. doi:[10.1007/s10533-015-0088-1](https://doi.org/10.1007/s10533-015-0088-1)
- Wagner, S., J. Brandes, A. I. Goranov, T. W. Drake, R. G. M. Spencer, and A. Stubbins. 2017. Online quantification and compound-specific stable isotopic analysis of black carbon in environmental matrices via liquid chromatography-isotope ratio mass spectrometry. *Limnol. Oceanogr. Methods* **15**: 995–1006. doi:[10.1002/lom3.10219](https://doi.org/10.1002/lom3.10219)
- Wagner, S., R. Jaffé, and A. Stubbins. 2018. Dissolved black carbon in aquatic ecosystems. *Limnol. Oceanogr. Lett.* **3**: 168–185. doi:[10.1002/lo12.10076](https://doi.org/10.1002/lo12.10076)
- Wagner, S., S. Brantley, S. Stuber, J. Van Stan, A. Whitetree, and A. Stubbins. 2019. Dissolved black carbon in throughfall and stemflow in a fire-managed longleaf pine woodland. *Biogeochemistry* **146**: 191–207. doi:[10.1007/s10533-019-00620-2](https://doi.org/10.1007/s10533-019-00620-2)
- Wagner, S., E. Harvey, N. Baetge, H. McNair, E. Arrington, and A. Stubbins. 2021. Investigating atmospheric inputs of dissolved black carbon to the Santa Barbara Channel during the Thomas fire (California, USA). *J. Geophys. Res. Biogeosci.* **126**: 1–17. doi:[10.1029/2021JG006442](https://doi.org/10.1029/2021JG006442)
- Wei, X., D. J. Hayes, and I. Fernandez. 2021. Fire reduces riverine DOC concentration draining a watershed and alters post-fire DOC recovery patterns. *Environ. Res. Lett.* **16**: 1–10. doi:[10.1088/1748-9326/abd7ae](https://doi.org/10.1088/1748-9326/abd7ae)
- Weishaar, J. L., G. R. Aiken, B. A. Bergamaschi, M. S. Fram, R. Fujii, and K. Mopper. 2003. Evaluation of specific ultraviolet absorbance as an indicator of the chemical composition and reactivity of dissolved organic carbon. *Environ. Sci. Technol.* **37**: 4702–4708. doi:[10.1021/es030360x](https://doi.org/10.1021/es030360x)
- Wiedemeier, D. B., and others. 2015. Aromaticity and degree of aromatic condensation of char. *Org. Geochem.* **78**: 135–143. doi:[10.1016/j.orggeochem.2014.10.002](https://doi.org/10.1016/j.orggeochem.2014.10.002)
- Williams, A. P., J. T. Abatzoglou, A. Gershunov, J. Guzman-Morales, D. A. Bishop, J. K. Balch, and D. P. Lettenmaier. 2019. Observed impacts of anthropogenic climate change on wildfire in California. *Earth's Future* **7**: 892–910. doi:[10.1029/2019EF001210](https://doi.org/10.1029/2019EF001210)
- Williamson, J. L., and others. 2021. Landscape controls on riverine export of dissolved organic carbon from Great Britain. *Biogeochemistry* **2**: 163–184. doi:[10.1007/s10533-021-00762-2](https://doi.org/10.1007/s10533-021-00762-2)
- Wozniak, A. S., A. I. Goranov, S. Mitra, K. W. Bostick, A. R. Zimmerman, D. R. Schlesinger, S. Myneni, and P. G. Hatcher. 2020. Molecular heterogeneity in pyrogenic dissolved organic matter from a thermal series of oak and grass chars. *Org. Geochem.* **148**: 104065. doi:[10.1016/j.orggeochem.2020.104065](https://doi.org/10.1016/j.orggeochem.2020.104065)
- Xu, C., Y. Xue, Y. Qi, and X. Wang. 2016. Quantities and fluxes of dissolved and particulate black carbon in the Changjiang and Huanghe Rivers, China. *Estuar. Coast.* **39**: 1617–1625. doi:[10.1007/s12237-016-0122-0](https://doi.org/10.1007/s12237-016-0122-0)

### Acknowledgments

We thank the City and County of Santa Cruz (Ezekiel Bean, Ryan Bassett, Lindsay Neun), NOAA (Rosealea Bond, Joe Kiernan), and California State Parks for their contribution of flow data and/or site access. We thank Peter Willits and Alicia Paez for help with sampling and Colin Carney for help with analyses. This research was supported by the National Science Foundation (Award #2101885), and both the Rensselaer Graduate Fellowship and CUAHSI Pathfinder Fellowship (to RB). We acknowledge the support from ASLO and Wiley in the form of an APC waiver offered to RB via the L&O Letters Early Career Publication Honor.

Submitted 01 June 2023

Revised 15 September 2023

Accepted 18 September 2023